2009-01-3184

New Blind, Doweling, Temporary Fastener Design and Testing

Samuel O. Smith
Electroimpact Inc

Travis McClure
Centrix, LLC

ABSTRACT

Several new families of expanding mandrel type of temporary (slave) fastener are in production and/or undergoing qualification tests. These fasteners are characterized by a collapsible mandrel that expands when needed over a center spindle. These fasteners are blind (installed and removed from one side only), and they provide locating (dowel) capabilities. This paper illustrates how these new fasteners work and how they are designed. Results of some testing of nominal ¼", flush head fasteners in carbon-fiber reinforced plastic are shown. Design criteria include the temporary fasteners clamping ability, acceptable contact stresses, cyclic fatigue life, and strength.

INTRODUCTION

The design of single-sided (blind), temporary (slave) fasteners (SSSF) has evolved, resulting in more potential use in aerospace manufacturing. SSSF are

- installed
- clamped
- loosened
- and removed

from the same side of the structure. See Figure 1 below.

SSSF are characterized by a collapsible mandrel that expands when drawn over screw thread and/or bushings. These fasteners are "blind" installed and removed (from the head side only) with wrenches or other simple torque tools. As shown in Figure 2 below, SSSF provide locating (dowel) capabilities.

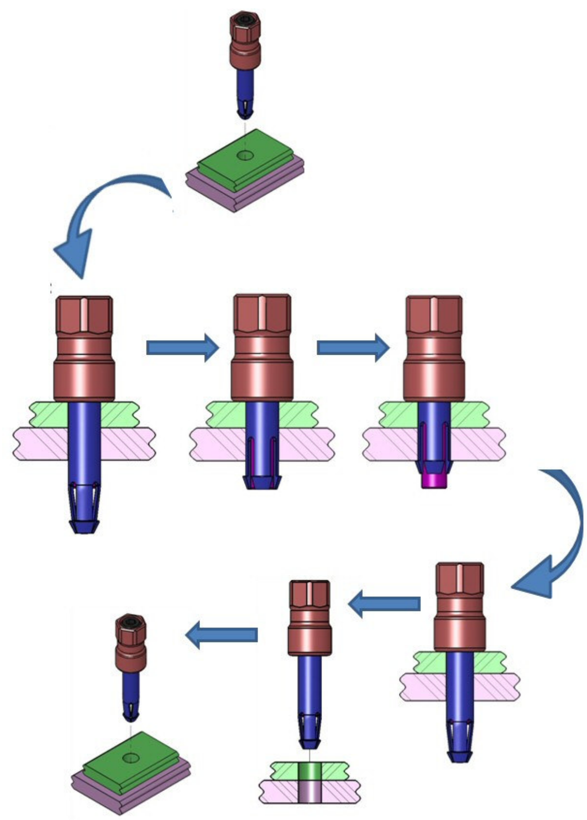

Figure 1. Using a single-sided slave fastener

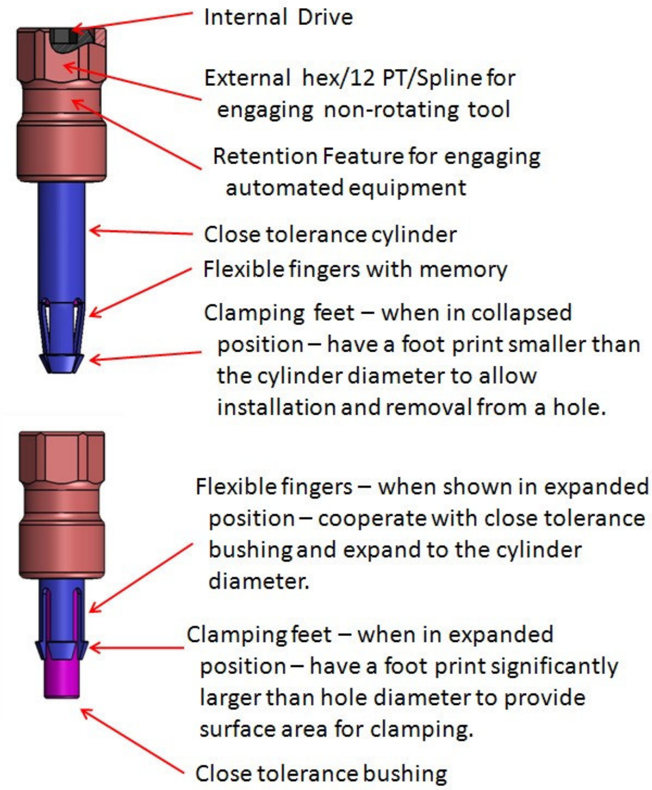

Figure 2. Important features of SSSF

There are many commonly used blind, temporary, removable fasteners used in aerospace manufacturing, including Cleco and other proprietary designs. Please see References 1 and 2. Fastener manufacturers are now making temporary fasteners to reduce delamination risk in composite materials. (Please see SAE paper 2008-01-2290, Reference 3.)

The newer SSSF discussed in this paper have the ability to closely locate (dowel) stacks of parts and clamp them together with larger forces than other temporary fasteners. Some examples of SSSF are shown in Figure 3, 4,and 5 below.


Figure 3. Photographs of some SSSF designs

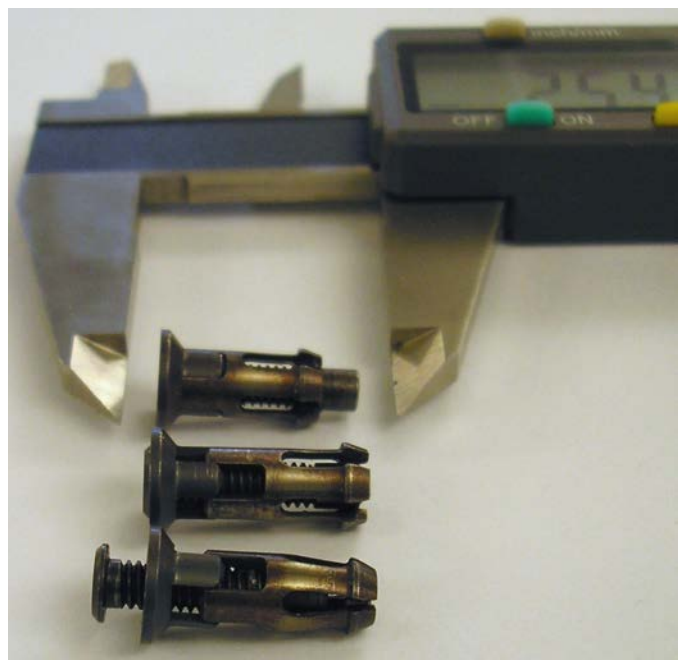
Figure 4. Photograph of Ø1/4 flush head SSSF design – side view

Figure 5. Photograph of Ø1/4 flush head SSSF design – tail isometric view

SSSF USE, DESIGN, AND TESTING

ASSEMBLY PROCESSES WITH SSSF – The capabilities of SSSF enable a variety of improved manufacturing processes. This is particularly true for situations allowing access from only one side of the assembly (blind assembly) and areas that need high clamping load during assembly. Benefits of using SSSF include the following:

- SSSF align (dowel) close tolerance parts.
- High clamp loads stabilize the assembly.
- High clamp loads do not damage the structure.
- Need to access only a single side of the assembly.
- Better accuracy maintains location of components during other assembly processes.
- High clamp loads reduce interlaminate burr.
- Repeatedly locates without a supporting jig.

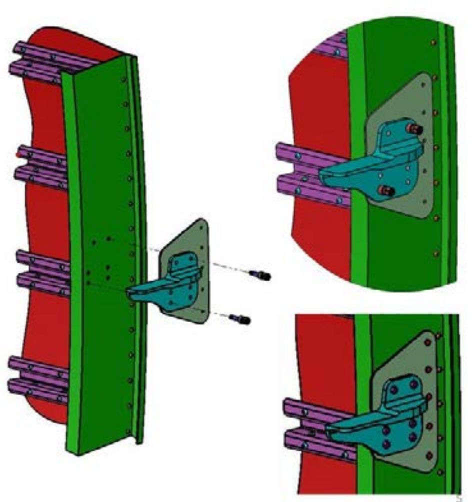

Figure 6 – Assembly example with SSSF

Determinant Assembly Example with SSSF – There is increasing aerospace use of parts with full sized, finished, CNC located holes (coordination holes). These can be matched up to other structure also having exact coordination holes.

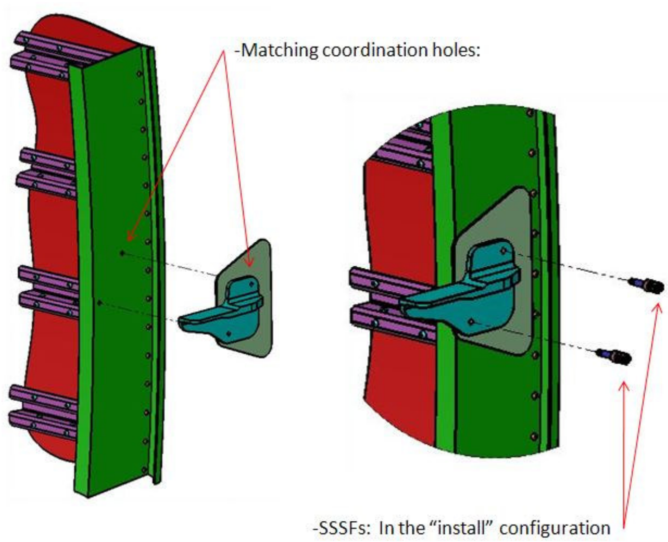

Figure 7 – Initial location during determinant assembly

SSSF are designed to easily install through the coordination holes, expand on the back side of the stack, and then apply clamp force via the application of torque. To remove the SSSFs, impart torque of equal magnitude in the opposite direction. The SSSFs will return to their “installation” configuration for removal, see the next Figure.

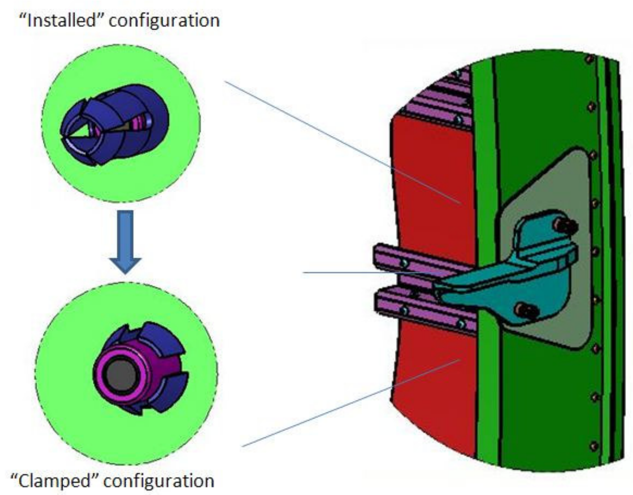

Figure 8 – Tail configuration of SSSF in a determinant assembly

In this determinant example, secondary drilling is required; the high clamp load and alignment of the SSSF provides a stable stack for drilling.

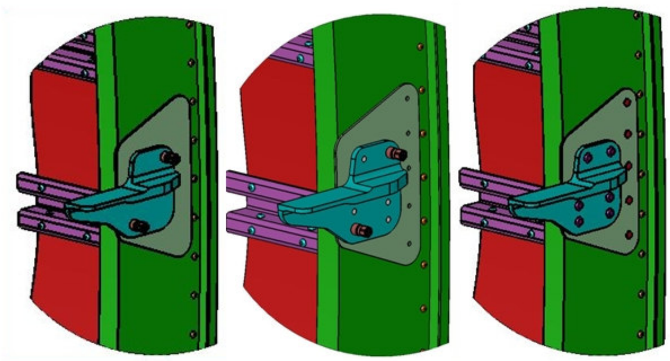

Figure 9 – Sequence of determinant clamp with SSSF, drill, and final fastening

Assembly with SSSF avoids some of the difficulties encountered with the following two examples of manufacturing. In the Figure 10, you must have access to the back side of the parts to use physical clamps or two-piece fasteners.

Figure 10 – Traditional: A part with pilot holes is clamped into position, not single-sided fastening

The example of Figure 11 requires more than 100, Cleco-type, temporary fasteners to provide sufficient clamping force and hole alignment.

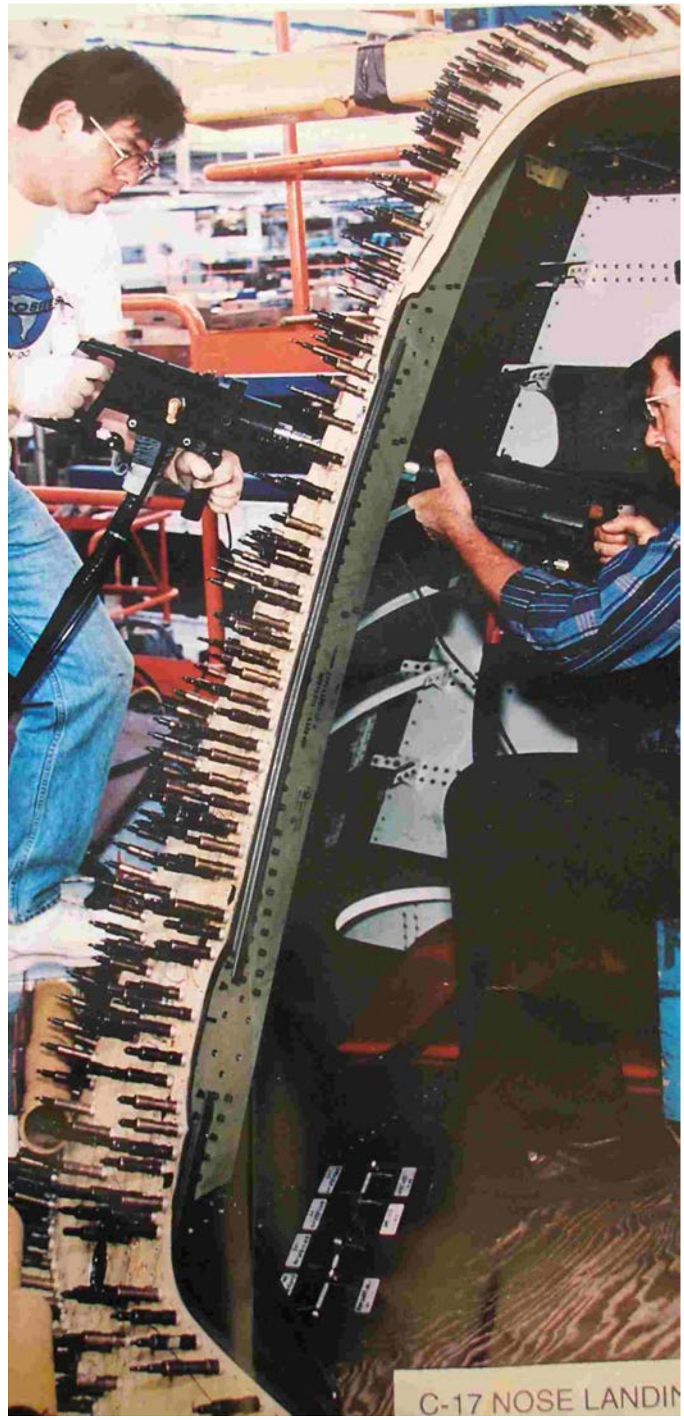

Figure 11 – Traditional: Many low-clamp force Clecos are needed for sufficient clamping (C17 nose landing gear door frame).

Wing assembly SSSF example – The following Figures 12, 13, and 14 show an example of a structural build of an outer sing box. SSSF allow construction of the rib/spar/skin matrix with many fewer temporary fasteners.

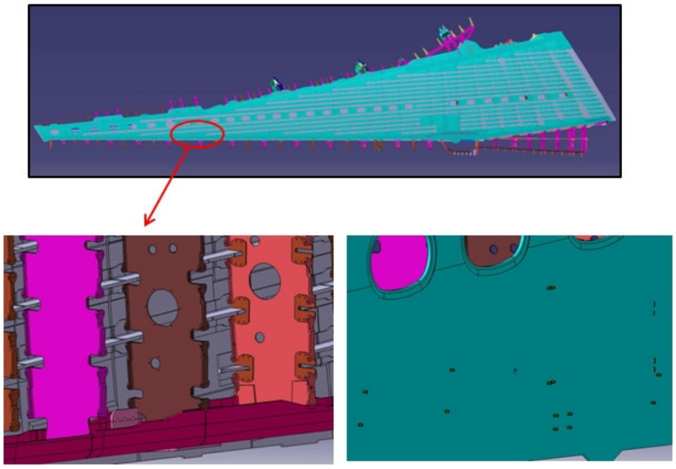

Figure 12 – Outer wing box build overall.

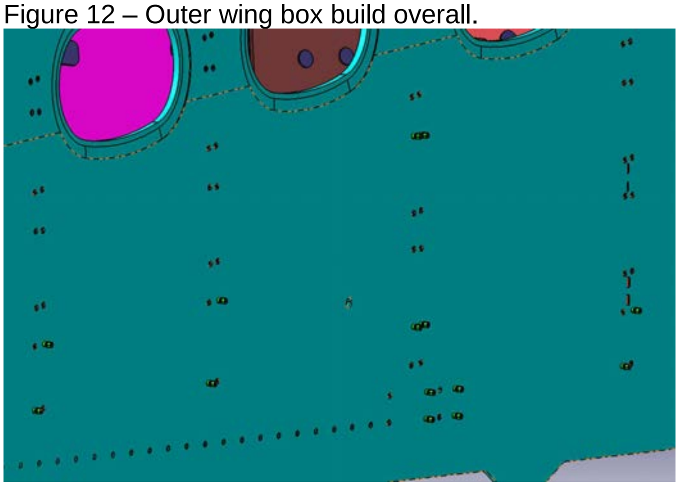

Figure 13 – Outer wing box build SSSF and drilled hole close-up.

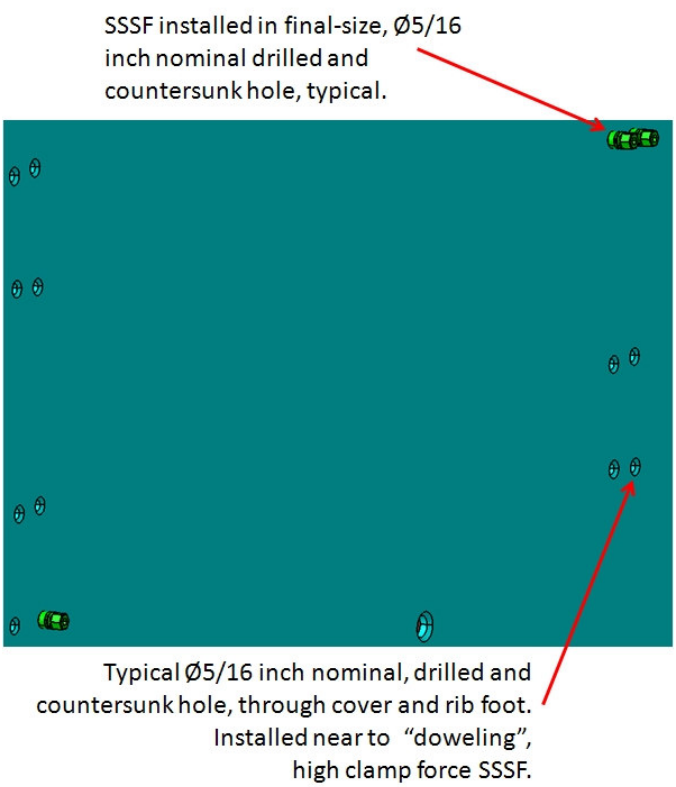

Figure 14 – Outer wing box build SSSF and drilled hole detail.

Compare the relatively few SSSF needed to adequately clamp and dowel this wing box together to the more traditional wing build wherein nearly every hole needs a dowel pin or a Cleco-type fastener; please see Figures 15 and 16.

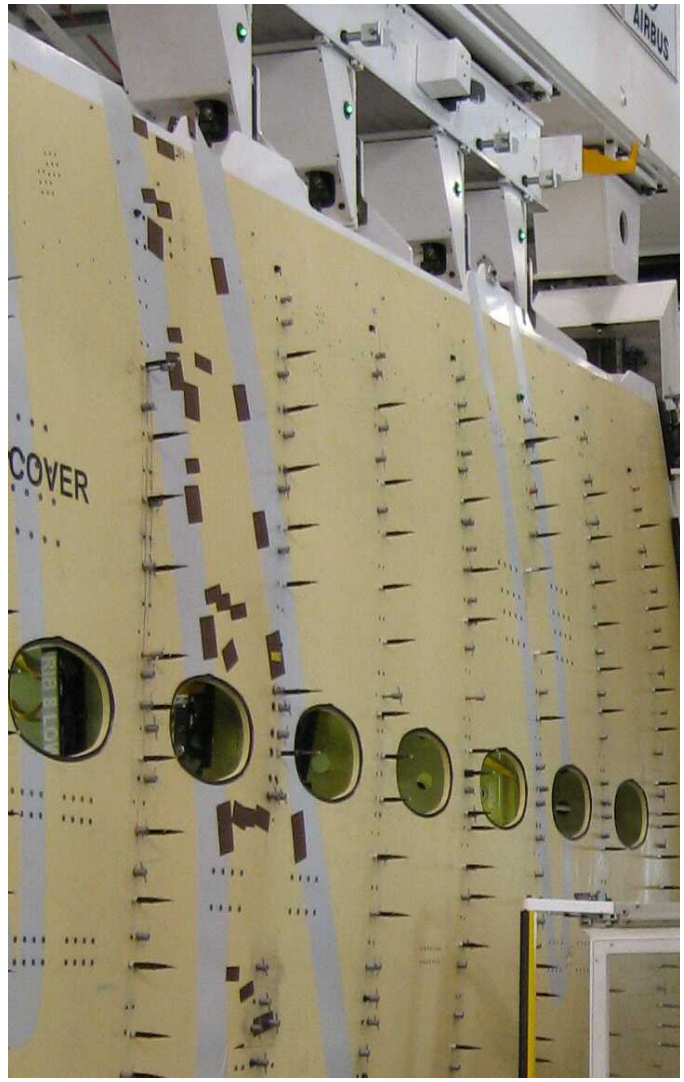

Figure 15 – Traditional outer wing box build using dowel pins and Cleco-type fasteners.

Figure 16 – Traditional outer wing box close-up using dowel pins and Cleco-type fasteners.

Advantages of using SSSF compared to traditional Cleco-type and dowel pins include the following:

- high clamp loads
- doweling
- Structure is drilled and indexed to the same holes (with the same tolerances) where the final, fly-away fasteners will later be inserted.
- Removable SSSF do not cause damage on the tail side of the CFRP structure.

SSSF FUNCTION, DESIGN, AND ANALYSIS OF FLEXIBLE METAL FINGERS - A key component of this design is to insure that the flexing fingers are capable of opening from an “installation” position, transferring a large clamp force, and then closing again prior to removal. This must be repeated for many cycles. To help determine if the fingers have enough memory to operate through multiple full cycles, non-linear FEA analysis was used and validated by comparing to test data.

First, a cad model of the collet body was created in the “machined” condition.

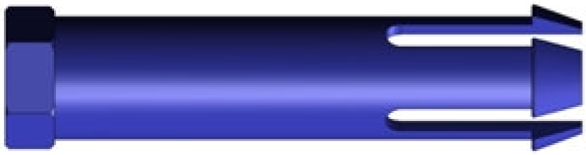

Figure 17. Machined collet body.

A “deform” feature was used in the cad program to simulate the formed shape of the collet body with the fingers being closed. In reality, the fingers are held in this position during heat treatment.

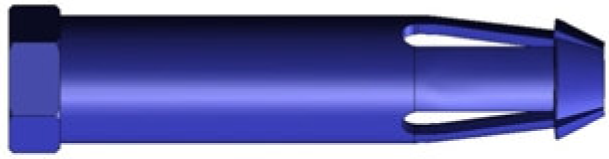

Figure 18. Fingers deformed as after heat treat.

With the basic collet body created, it was just a matter of creating a few more components and sectioning for symmetry. In the figure below, the hole is represented by a yellow cylinder, and all bodies are sectioned into quadrants along symmetry planes.

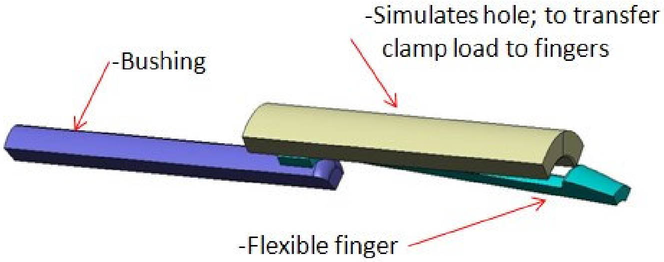

Figure 19. Sectioned flexible finger, bushing, and hole models

With the cad model created, a FEA model was developed to apply axial movement of the internal bushing to open the flexible fingers, apply load to the fingers through geometry simulating the hole, and completely reversing the cycle to ascertain the residual state of the flexing fingers. This was done by setting the models (Case 1, Case 2, and Case 2A) to run as a function of time. In other words, at time=0 seconds, the model resided in its neutral state as shown above. As time progressed, forced displacements and loads are progressively applied until maximum values are reached at time=0.5 seconds. After which the impetus of the loads and forced deflections are reversed and progressively diminish to a value of 0 at time=1.0 seconds. This also allows the staging of loads and deflections. For instance, the bushing can be put into motion until it reaches it appropriate position while the loads remain 0. Once in position, the bushing stays in position while the loads are cycled from 0 to max to 0 again. After a full cycle of loading, the bushing is then again put into motion so that it returns to its original position thus leaving the model in a completely cycled state – making all residual measurement possible. In addition, a full material curve – plastic and elastic – was used for the fingers. This allows strain hardening, redistribution of stresses and loads during yielding, and depicts the residual state of the material after a complete cycle. Also, all contacting geometry within the model elements are updated as a function of time. As boundary condition change due to deflections, so do the load paths and stresses. Lastly, all nodes are tracked as a function of time so that each node can be mined for any information associated with the analysis.

Prior to reviewing the analysis, it is important to examine the geometry of a curved beam with transitional radii, and being bent at said radii.

As shown below, the base of the beam is depicted in Section A. Section planes B and C are progressively farther away from the base of the beam. As shown in Figure 21, the cross-sectional areas progressively diminish with increasing distance from base Section A. This continues until Section C – after which the cross section remains constant. Also notice that the extreme fiber distances from the neutral axis follow a similar pattern – highest values in section Section A, and lowest in Section C.

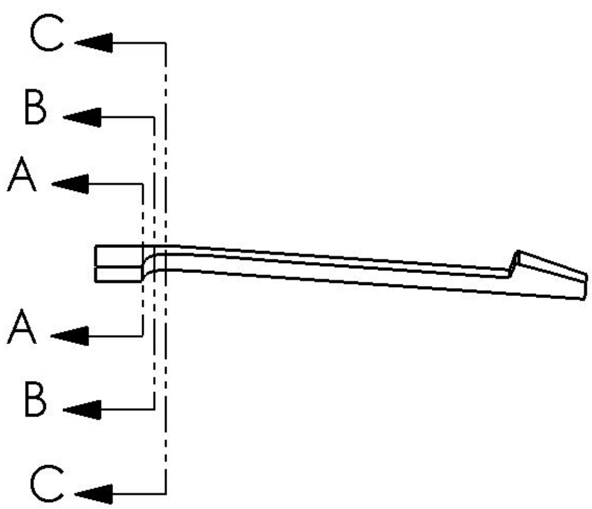

Figure 20. A single finger shown in the post heat treat condition depicted with multiple section planes.

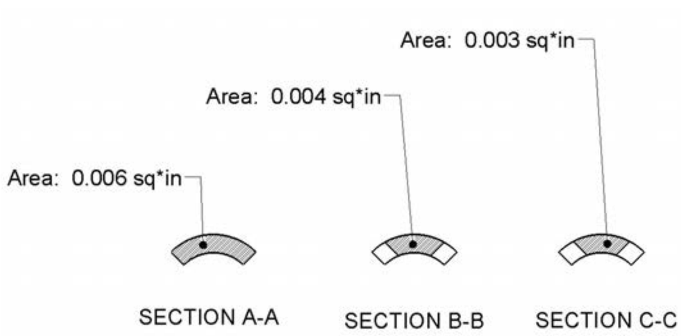

Figure 21. A single finger for a typical Ø 1/4 inch SSSF is shown in the post heat treat condition; multiple section planes are shown.

In use, the SSSF's fingers are subjected to combined loading. Bending stresses are incurred during installation when the fingers are pulled over the center spindle, forcing the fingers from a closed position to an open position – effectively bending the fingers open. More tensile stress is incurred when the SSSF is torqued to create clamping forces (clamp-up). As such, tensile stresses from bending accumulate with the tensile stresses from axial loading, and subtract on the compressive side of the beam.

As with all cantilevered beams in bending, the greatest moment occurs at the base of the beam from which it is fixed. In this case, Section plane A represents the greatest moment. It also has the greatest extreme fiber distance, and the largest centroidal moment of inertia. Section A-A also has the largest area thus having the least tensile stresses from the axial loading component. As mentioned above, these ratios change progressively as the distance from Section plane A increases. In this case, it is ideal to use FEA analysis to study the effects of so many convergent factors.

To examine the performance of the finger, three models where compared and contrasted.

Case 1 - Fingers open and close for a typical Ø 1/4 inch SSSF. This model represents the behavior of the fingers from just being opened and closed.

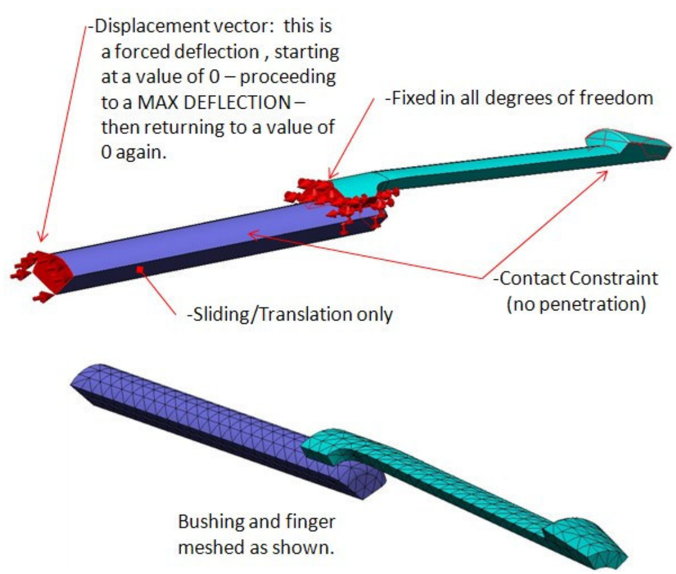

Figure 22. FEA constraints for fingers opening and closing.

In this analysis, at time=0 seconds, the model resided in its neutral state as shown above. At time=0.5 seconds, the bushing has been fully positioned so that the finger is flexed open. At time=1.0 seconds, the bushing has fully retracted to its starting position. The results below show the stress state when the fingers are fully opened. This is half way through the analysis. In this analysis, the results predictably show high tensile stresses at the lower corner, and high compressive stresses at the top of the curved beam.

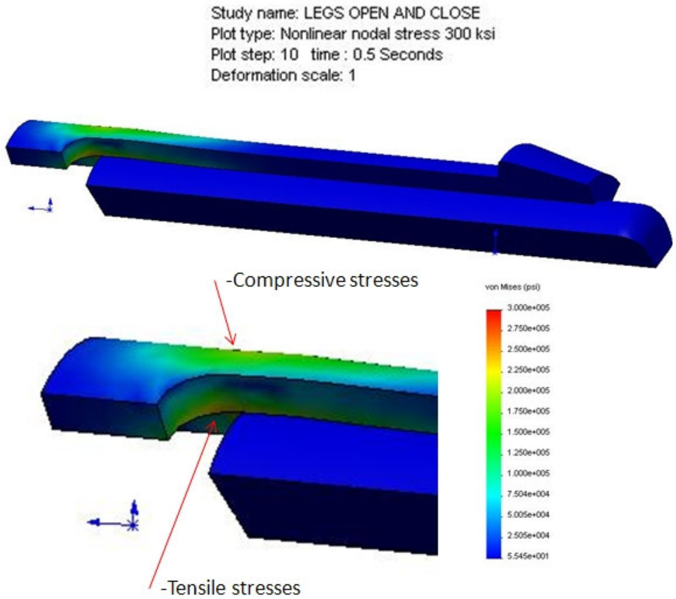

Figure 23. Stresses when fingers open

The results below show the stress state of the flexible finger after being fully opened and allowed to close without restraints. This is at the end of the analysis, showing the residual stress state. No residual stresses are present as the material did not go into yielding.

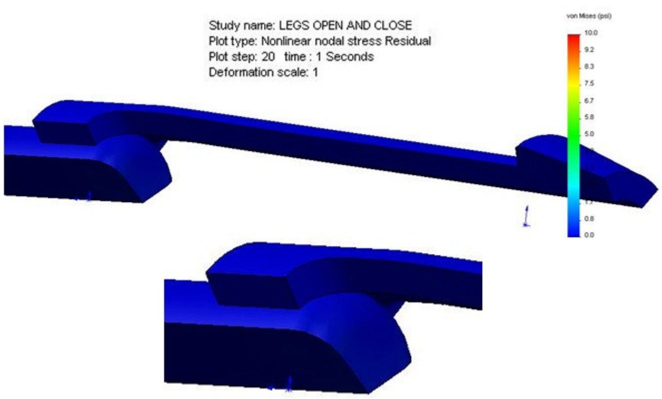

Figure 24. Case 1 loading does not cause residual stress or deflection after fingers close

Case 2 – Fingers opened, loaded in tension, and closed in a typical Ø 1/4 inch SSSF. The model and analysis below represents the behavior of the fingers as they are opened, loaded in tension, unloaded and allowed to close.

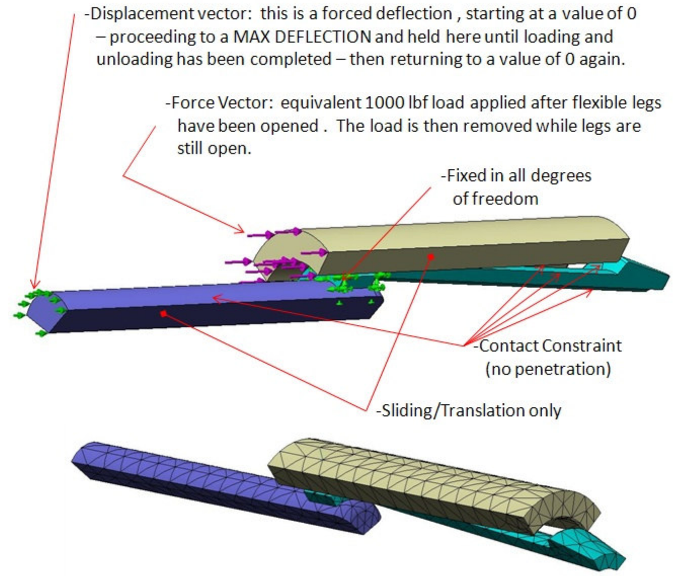

Figure 25. Model and meshing for Case 2 loading

In this analysis cycle, at time=0 seconds, the model resided in its neutral state as shown above. At time=0.25 seconds, the bushing has been fully positioned so that the finger is flexed open. At time=0.26 seconds, the load is activated, and reaches its maximum value at time=0.5 seconds, and diminishes to a value of 0 at time=0.74 seconds. At time=0.75 seconds, the bushing begins to return to its original position and continues to do so until time=1.0 seconds at which the bushing has fully retracted to its starting position.

Figures 26 - 28 below shows the stress state when the fingers are fully opened, and an equivalent load of 1000 lbf (4448 N) is applied as of the fastener in clamping. This is half way through the analysis cycle. The figures depict the accumulation of the stresses from the clamping force and the stresses generated from opening the legs. Notice that the stresses are around the yield point for the material.

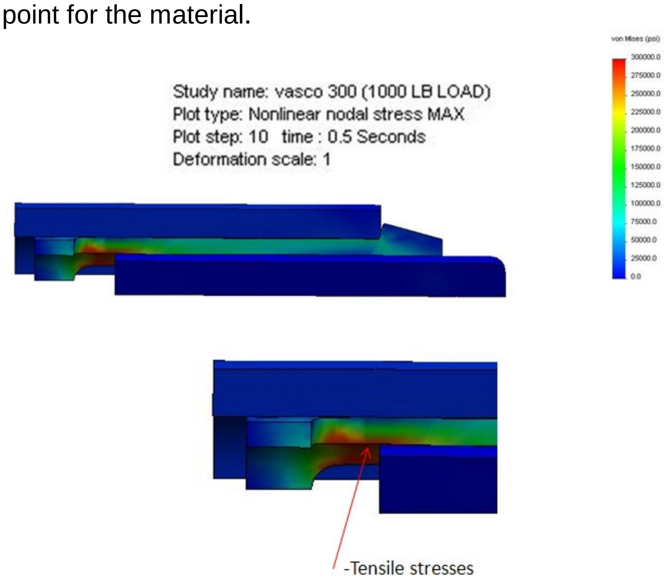

Figure 26. Maximum stresses during clamping.

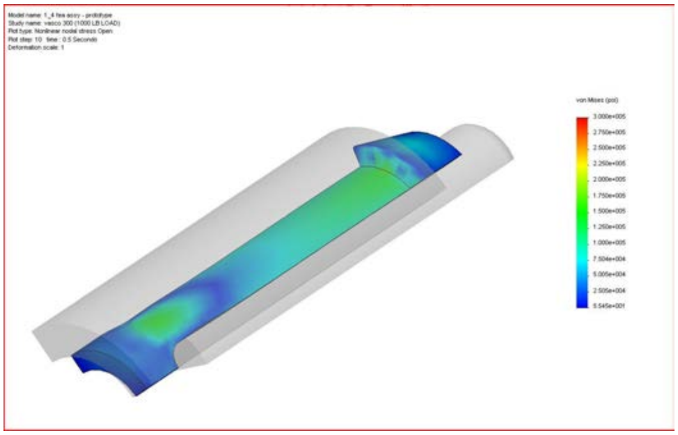

Figure 27. Maximum stresses during clamping – top view.

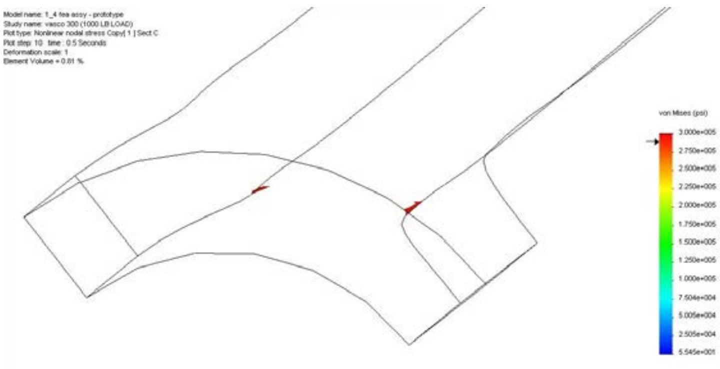

Figure 28. Volume of material that has exceeded yield levels.

Figure 29 shows the stress state after a complete cycle of fingers being opened, loaded, then unloaded, and allowed to close without any applied loads. This is at the end of the analysis, and is intended to show the residual stress state. Some minor residual stresses are present as the material did undergo yielding in small segment of material at the outer fringes of the curved beam.

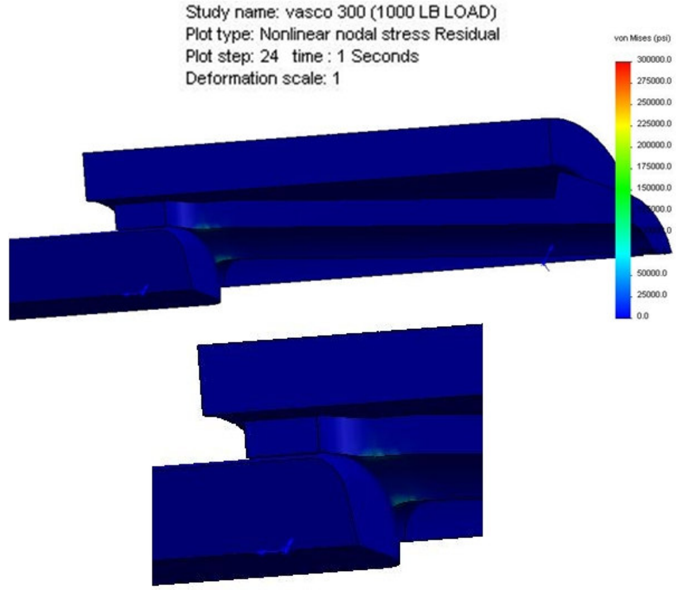

Figure 29. Residual stresses after Case 2 loading

The following figure is at the end of the analysis after Case 2 loading, and shows the residual deformed state. Residual stresses also go hand in hand with residual displacement. The Figure 30 shows 0.00025 inch (0.006mm) residual deformation at the tip of the finger. Notice that this level of residual deformation is negligible. As we shall see in the following section, actual fastener testing verifies these FEA results.

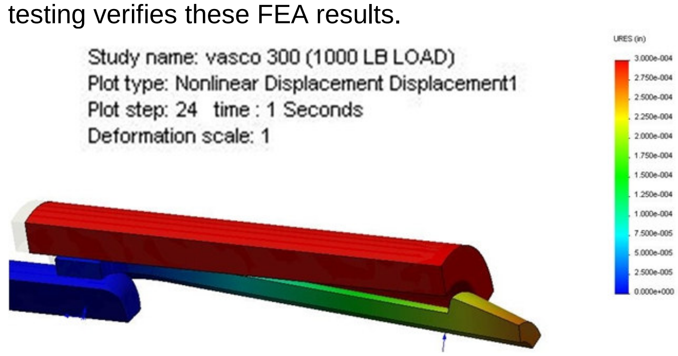

Figure 30. Residual deformation.

Case 2A: Behavior of fingers in extreme overload conditions for a typical Ø 1/4 inch SSSF. The analysis below represents the behavior of the fingers as they are opened, loaded in tension with a excessive force magnitude representing extreme usage, unloaded and allowed to close. Boundary conditions are the same as in Case 2.

Figures 31, 32, and 33 below show the stress state when the fingers are fully opened, and an equivalent load of 1600 lbf (7117 N) is applied as of the fastener in clamping. This is half way through the analysis. The figure depicts the accumulation of the stresses from the clamping force and the stresses generated from opening the legs. Notice that the stresses are around the yield point for the material.

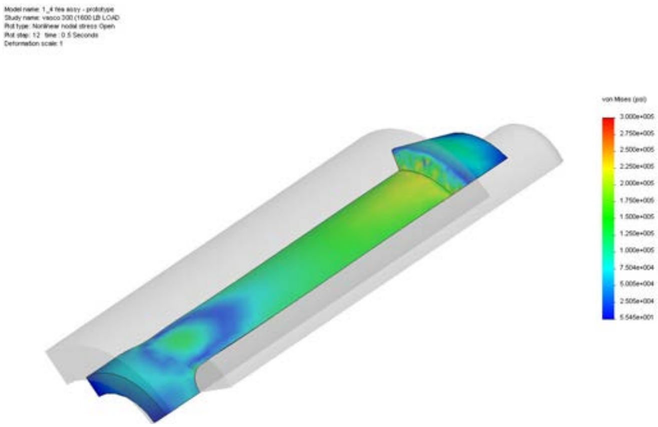

Figure 31. Maximum stresses during clamping – top view.

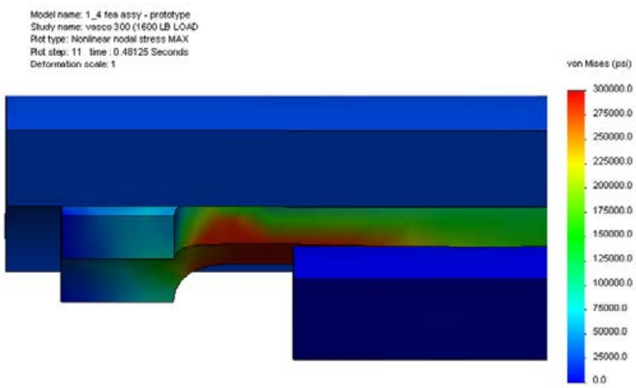

Figure 32. Maximum stresses during clamping.

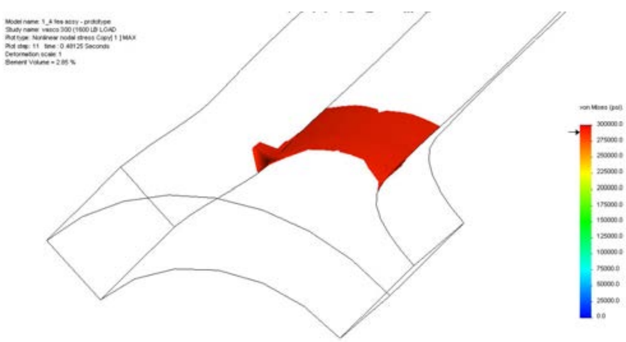

Figure 33. Volume of material that has exceeded yield levels during maximum clamping.

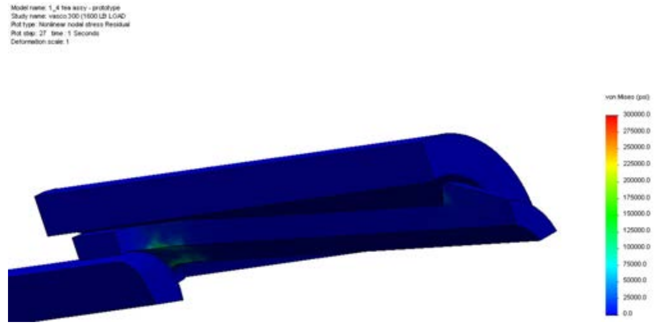

Figure 34. Residual stresses after Case 2A loading

As the previous figures show, Case 2A loading produces more yielding and more residual stresses than case 2. Figures 34 and 35, at the end of the analysis after Case 2A loading and unloading, illustrate the residual stresses and the residual deformed state. Residual stresses also go hand in hand with residual displacement. The figure shows 0.0025 inch (0.06mm) residual deformation at the tip of the finger.

Even at this level of residual deformation, the tool is still highly functional, and can be seen in the testing section.

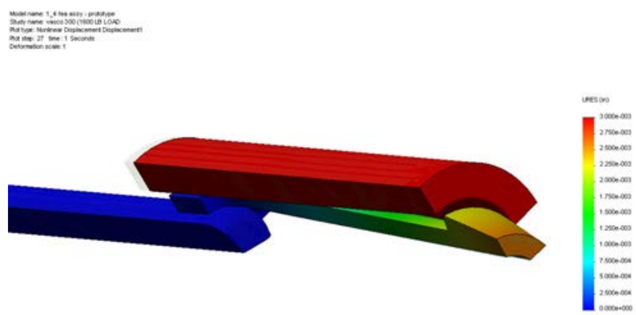

Figure 35. Residual deformation after Case 2A loading

As these analyses depict, the flexing fingers are capable of opening from an "installation" position, transferring a large clamp force, and then closing again prior to removal. As for a cycle analysis, actual testing will be relied upon in order to reach a conclusion. From a classical fatigue analysis approach, yield stresses should never be reached if any kind of fatigue life is to be assumed. Ideally, for infinite life in steels, less than %50 percent of the yield stresses should be the maximum design limit (depending on stress concentration, surface finish, etc.). However, as the following section will show, testing reveals that the flexing fingers do not fail in the areas of the transitioning radii.

VALIDATION OF FEA ANALYSIS - The above models and below testing is performed on a typical Ø 1/4 inch SSSF design – one requested by commercial aircraft production. The airframe manufacturer needed a fastener that would provide doweling and high clamp load without pulling though the aluminum skin. The following photographs show the SSSF installed between plates through a ring-type load cell.

The following testing was performed on the same Ø 1/4 inch SSF design as shown in the FEA analysis. The aim is to ascertain the correlation between analysis and actual performance of the SSSF.

Figure 36. Test setup. Load cell with digital readout, SSSF (Ø 1/4 inch), torque wrench. This is shown at the start of testing – fingers are only opened to trap the stack of 2 plates and the load cell.

Figure 37. The tool is torqued until the load cell reads approximately 1000 lbs (a little over to account for any error) which corresponds to the Load Case 2 in the FEA section.

Figure 38. The tool is reverse torqued until it returns to its neutral state. Notice that the fingers are touching at the tips. This suggests than no noticeable residual deformation has taken place, just as the FEA analysis predicted.

Figure 39. The tool is torqued until the load cell reads approximately 1600 lbs (a little over to account for any error) which corresponds to the Load Case 2A in the FEA section. This test is designed to push the fingers past their design point and compare to the FEA analysis.

Figure 40. The tool is reverse torqued until it returns to its neutral state. Notice that the fingers are now slightly separated at the tip. This suggests than residual deformation has taken place, just as the FEA analysis predicted. The distance across the bulges on the fingers measured 0.233 inches before the test, and measured 0.237 inches after the test. This is a change of .004 inches total, or .002 inches per side. The FEA model predicted 0.0025 inches per side. Some error is attributed to the difficulty of measuring flexible fingers that easily move – especially now that they are slightly separated. It is worth noting that the tool still easily exited the 1/4 inch hole in the structure, and was easily re-inserted back into the stack. As a practical matter,

SSSF are designed so the fingers in their natural state have plenty of clearance with respect to the hole.

PHYSICAL TESTING OF A FLUSH HEAD Ø 1/4 INCH SSSF DESIGN –Testing will include the following:

1. Clamp load versus torque
2. Ultimate torque and ultimate load tests
3. Cyclic, fatigue testing of the fastener
4. Checking for tail side damage around the hole in aircraft material

This particular SSSF design was request was for military aircraft production. The airframe manufacturer needed a flush head fastener for use in carbon fiber reinforced plastic (CFRP). They also required a fastener that would not damage CFRP when the fastener was tightened to its maximum value. The Ø1/4 inch nominal, 100° countersunk head fastener has a grip range of 0.490 to 0.635 inch (12.5 to 16.1mm). Please see Figures 4 and 5 above, and Figure 41 below.

Figure 41 Three, Ø1/4 inch, flush head SSSF, isometric view from the head side.

Physical testing, pull-up load versus torque – Electroimpact installed these fasteners in a “star” coupon and measured the clamping load as a function of the torque placed on the fastener’s internal drive screw. Testing conforms to NASM1312. See the figures below.

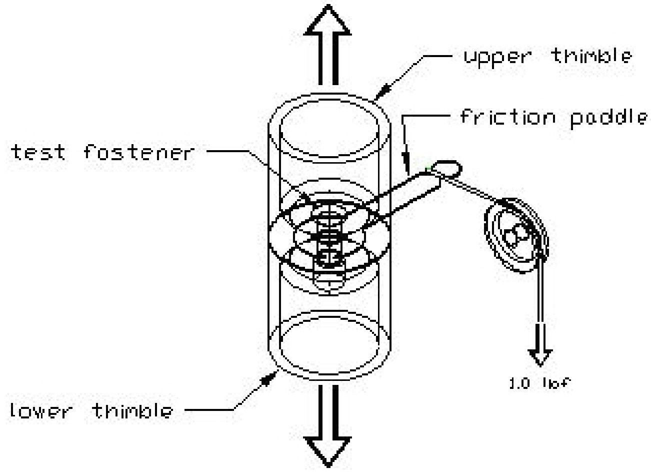

Figure 42. Tension testing per MIL-STD-1312-16

Figure 43. Star coupon testing in tension/compression machine.

Results of the clamp load versus torque testing is shown in Figure 44.

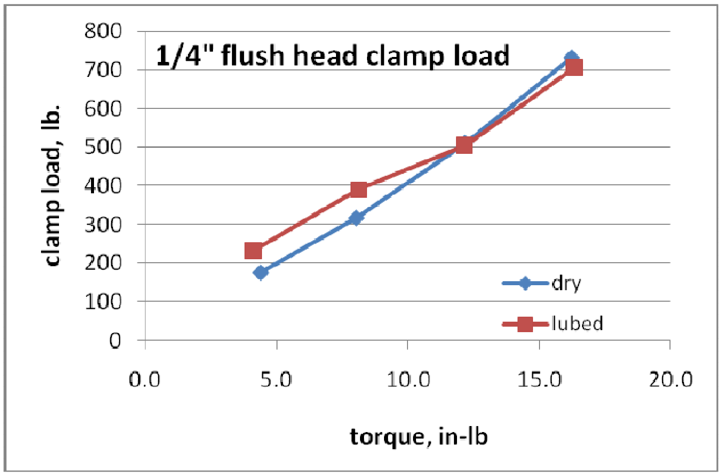

Figure 44. Clamp load versus torque for a Ø1/4, 100° countersunk SSSF.

Physical testing, ultimate torque and tension load – Electroimpact tested several of the Ø1/4, flush head, SSSF to failure. Sample1 reached 39 in-lb of torque, before the head of the internal screw came apart in tension. Sample 2 reached 32 in-lb of torque. That torque stripped the internal hex of the screw.
Sample 3 was minimally torqued and failed at 1030 lb (4580 N) of tension. The head of the fastener completely separated in this ultimate test.

Physical testing, cyclic fatigue of SSSF – A sample of the Ø1/4, flush head, SSSF installed in a star coupon on Electroimpact's fatigue test machine is shown in the following two figures. Sample 4 was minimally torqued, and had a tension load cycling between 150 and 510 lb (670 and 2370N). 550 cycles, no failure.

Sample 5 was minimally torqued, and had a tension load cycling between 100 and 678 lb (440 and 3020N). 505 cycles, no failure.


Figure 45. Fatigue test of a SSSF, head isometric view

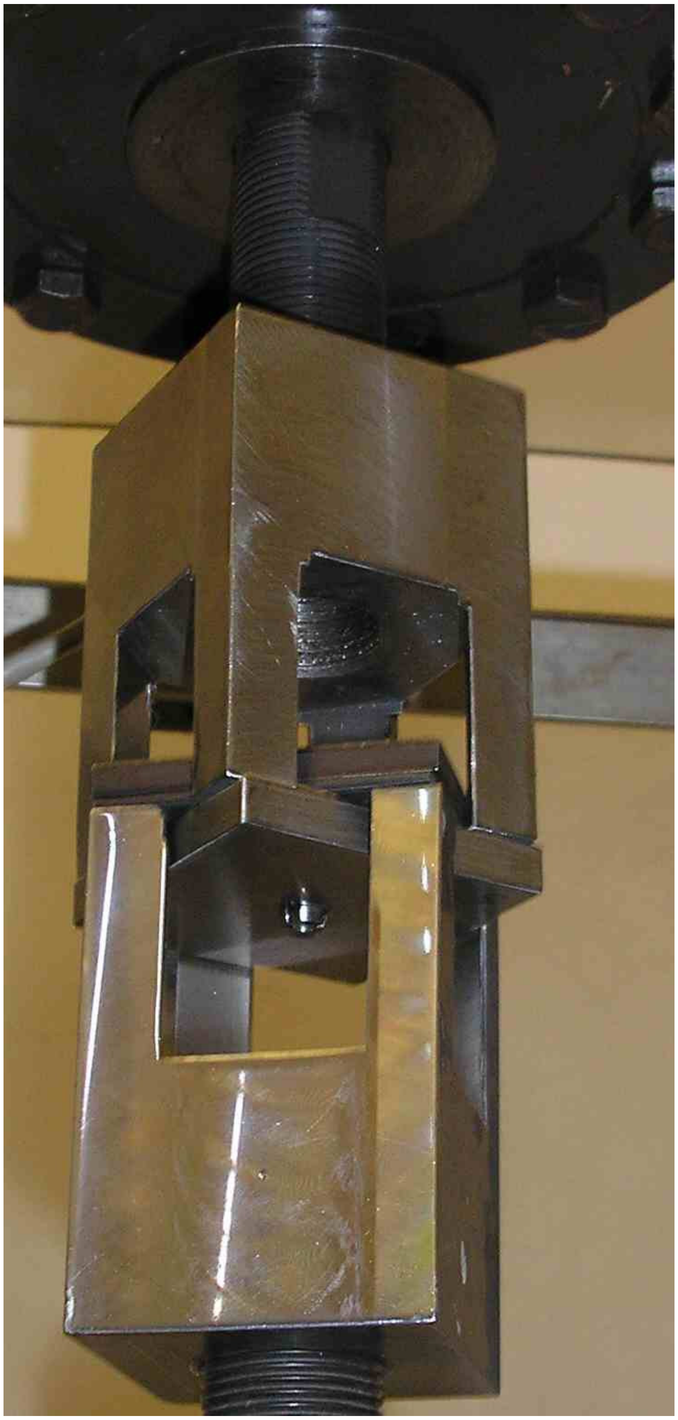

Figure 46. Fatigue test of a SSSF, tail isometric view

Physical testing, checking for tail-side damage - Several samples of Ø1/4 holes were pre-drilled in through CFRP. The samples of CFRP tested had a thin layer of fiberglass mesh on their surface to prevent delamination at drill bit breakthrough. The holes were photographed before, during, and after the SSSF installation. Compare the figures below.

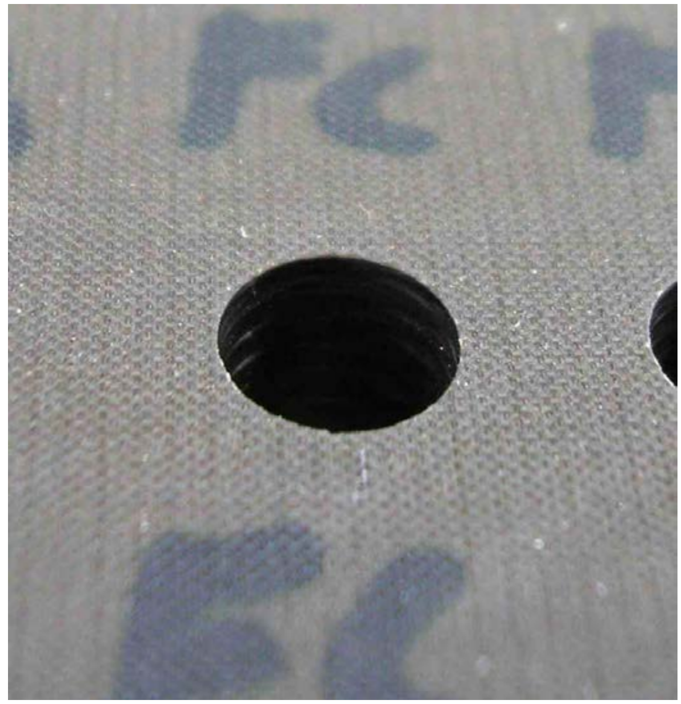

Figure 47. Tail-side hole specimen, before SSSF

Figure 48. Tail-side hole specimen, during SSSF installation at 20 in-lb of torque

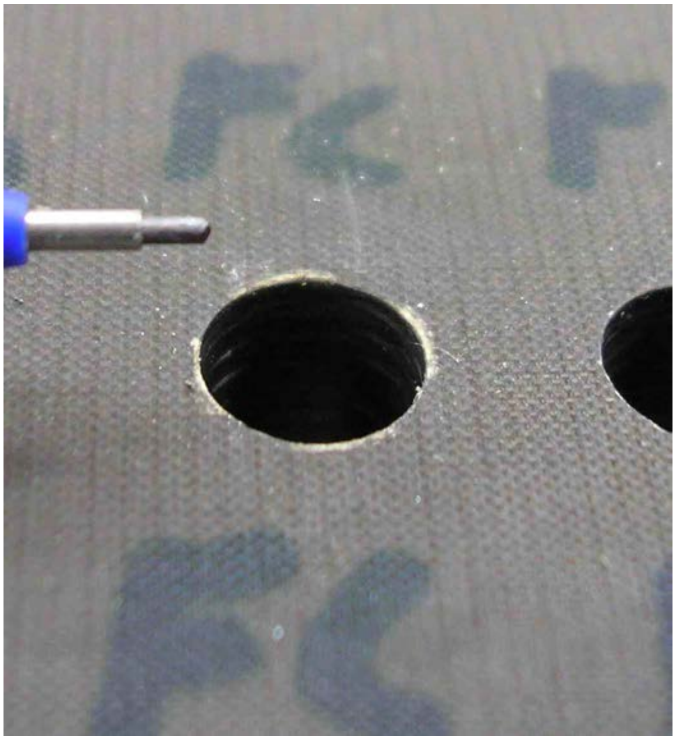

Figure 49. Tail-side hole specimen, after SSSF was installed with 20 in-lb of torque. Note: The pencil diameter shown for reference is 0.7mm (0.028 inch.)

20 in-lb (2.3 Nm) is 25% more torque than the maximum production torque value and corresponds to roughly 900 lb. (4000 N) of clamping load. Figure 49 shows that the SSSF causes only superficial cosmetic marks on the fiberglass layer.

CONCLUSIONS

Newer design single-sided slave fasteners (SSSF) have unique features that enable simpler aerospace manufacturing, including alignment (doweling), single-side insertion, and high clamping loads.

Key to the design of SSSF is the collapsing legs. These legs are curved metal beams. Finite element analysis correlates closely with the stress and deflections seen by actual SSSF design.

Testing of the torque, clamp-up force, fatigue testing, and ultimate load of SSSF design allows their use with appropriate safety factors. Close-up photographs reveal no significant damage by the tail-side of SSSF pulling on CFRP material.

REFERENCES

1. Proprietary single-sided fastener for composite structures, see http://www.alcoa.com/fastening_systems/aerospace/en/pdf/Ergo-Tech_Flyer_5_05.pdf
2. Proprietary single-sided fastener for composite structures, see http://www.monogramaerospace.com/files/active/0/DAD%20SEPT2008.pdf
3. 2008-01-2290, “A New Concept of a Temporary Fastener for Composite Structures”, by Dieter Jüling, Marcus Scheinberger, and Luke Haylock, all of Alcoa Fastening Systems, SAE AMAF, Conference. See also http://www.sae.org/mags/AEM/6131, SAE’s Aerospace Engineering and Manufacturing Online, 25-Mar-2009.

CONTACTS

To inquire about stock or custom single-sided, slave fasteners, contact Travis McClure the President of Centrix, llc. Telephone (001) 206-909-3773, mailto:travis@centrix-llc. Their web site is www.Centrix-LLC.com

Samuel O. Smith is a Project Engineer with Electroimpact Inc. Telephone 425-609-4892, email sams@electroimpact.com, web site www.electroimpact.com

DEFINITIONS, ACRONYMS, ABBREVIATIONS

CFRP: carbon-fiber, reinforced plastic
SSSF: single-sided (blind), slave (temporary) fastener